Improving the Fretting Biocorrosion of Ti_6Al_4V Alloy Bone Screw by Decorating Structure Optimised TiO_2 Nanotubes Layer

Jiajun Luo[1], *Maryam Tamaddon*[1], *Changyou Yan*[2], *Shuanhong Ma*[2*], *Xiaolong Wang*[2], *Feng Zhou*[2], *Chaozong Liu*[1*]

[1]Institute of Orthopaedic & Musculoskeletal Science, Division of Surgery & Interventional Science, University College London, Royal National Orthopaedic Hospital, Stanmore, HA7 4LP, United Kingdom

[2]State Key Laboratory of Solid Lubrication, Lanzhou Institute of Chemical Physics, Chinese Academy of Sciences, Lanzhou, 730000, China

Corresponding author: chaozong.liu@ucl.ac.uk ; mashuanhong@licp.cas.cn;

Highlights:

Structure optimised TiO_2 nanotubes layer was generated on the surface of Ti_6Al_4V medical grade bone screws, the fretting and corrosion performance of TiO_2 nanotube decorated screw was investigated on a fretting test jig. The experiments have demonstrated that the structure optimised TiO_2 nanotube decorated Ti_6Al_4V bone screw exhibited an reduced the fretting wear and improved biocorrosion resistance.

Abstract:

TiO_2 nanotubes (NT) has been demonstrated its potential in orthopaedic applications due to its enhanced surface wettability and bio-osteointegration. However, the fretting biocorrosion is the main concern that limited its successfully application in orthopaedic application. In this study, a structure optimised thin TiO_2 nanotube (SONT) layer was successfully created on Ti_6Al_4V bone screw, and its fretting corrosion performance was investigated and compared to the pristine Ti_6Al_4V bone screws and NT decorated screw in a bone-screw fretting simulation rig. The results have shown that the debonding TiO_2 nanotube from the bone screw reduced significantly, as a result of structure optimisation. The SONT layer also exhibited enhanced bio-corrosion resistance compared pristine bone screw and conventionally NT modified bone screw. It is postulated that interfacial layer between TiO_2 nanotube and Ti_6Al_4V substrate, generated during structure optimisation process, enhanced bonding of TiO_2 nanotube layer to the Ti_6Al_4V bone screws that leading to the improvement in fretting corrosion resistance. The results highlighted the potential SONT in orthopaedic application as bone fracture fixation devices.

Keywords: Bone implant interface; Bone screws; Biomedical materials; TiO_2 nanotubes; Fretting corrosion;

1. Introduction

Titanium-based alloy implants have been widely used for various types of bone-anchored reconstructions due to their excellent mechanical properties and the several nanometer thick oxide film that featured with a successful biocompatibility and corrosion resistance [1]. This naturally formed oxide layer is bio-inert, which is not conducive to bonding at bone-implant interface [2]. Vertically aligned anodic NT have attracted much attention for their biofunctions, the improvement of osteointegration by acceleration of mesenchymal stem cells (MSCs) osteogenic differentiation [3-6]. Moreover, the remarkable antibacterial activity of NT was also documented [7, 8]. The in vivo animal models including mini pigs, rabbits and rats have all well demonstrated that NT has positive biofunctional abilities [9-11]. However, the implant used in human is different from that used in the animals as it needs higher biomechanical stability due to the significant extended service *in vivo*. In fact, the weak bonding strength of nanotubes to the substrate has been documented, i.e. the nanotubes layer can debonding easily from titanium substrate when subject to stress [12, 13]. The debonding of nanotubes will generate debris and could leading to integration failure at the bone-implant interface. Furthermore, clinical retrieval reports mention that wear debris can cause mild and severe tissue reactions [14, 15]. In typical case, the micro-movement between nanotube layer and the substrate when the implant is inserted into the human body, i.e. fretting will happen. This plays a vital role for the failure of bone-implant interface. Wear particles generated by fretting lead to inflammation and bone resorption, and prevent osteointegration [16]. Apart from fretting wear, fretting-induced corrosion phenomenon is also another dominant factor for implants degradation. Clinically, titanium implants are surrounded by blood-rich tissue, with the serum proteins in the blood possibly affecting implants corrosion behavior. Correspondingly, synergetic contribution from fretting wear and fretting corrosion that occurs at the bone-implant interface is an irreversible process that finally leads to failure of the bone implant [17, 18].

The clinical orthopaedic and dental devices are mostly designed with sharp curved surfaces, such as screw thread. These diverse surfaces cause a more complicated stress distribution on implants surface. Retrieved bone screw examinations revealed server worn thread as a result of fretting, and leading to the mechanical failure of the bone screw. To improve the fretting resistance, we have developed a novel SONT layer on bone screw surface

by creating a interfacial layer between TiO2 nanotube and the substrate. The fretting test was performed by using a self-built test platform to evaluate the anti-wear behavior of resulted SONT, compared with that of pristine bone screw and conventionally NT modified bone screws. In addition, the biocorrosion behavior of the NT and SONT decorated bone screws were also evaluated by monitoring the open circuit potential (OCP) value in simulated body fluid (SBF). The experiment results indicate that screws decorated with both NT and SONT layer exhibited reduced wear and improved anti-corrosion behavior when compared with a pristine machined bone screw (MA). Meanwhile, screw decorated with SONT layer showed much higher wear and corrosion-resistance behavior than that of screw decorated with NT layer. It is postulated that the improvement of fretting corrosion resistance of SONT layer could be attributed to the improvement in interface bonding, that provide a protection effect to the substrate. To our knowledge, this provides the first insight on fretting corrosion behavior of NT and SONT on alloyed orthopaedic screws countering with bone.

2. Materials and Methods

2.1 Generate conventional and structure optimized TiO_2 nanotube on screws

Ti_6Al_4V medical grade (TC4) veterinary fixation screws (3.5 mm major diameter and 26 mm length, self-tapping screw, Shanghai Huifu manufacturing Co., Ltd) were used in this study for generate NT and SONT modified bone screws. For surface modification, the screws were sequentially cleaned in ultrasonic cleaner for each 15 min with acetone (99.5%, Fisher Scientific), ethanol (99.8%, Fisher Scientific), and deionized (DI) water, then air-dried. The anodization was first performed in ethylene glycol (EG, 99.5%, ACROS Organics) with 0.5 wt% NH_4F (98%+, ACROS Organics) for 30 min under 60 V voltage, to obtain conventional NT modified screws. Followed by the first anodization, the screws were further anodized in EG solution with 3 wt% H_3PO_4 (85%+, Fisher Chemical) for 1 min under 60 V to obtain SONT. The screws were then rinsed with DI water and dried with N_2 stream. NT fabrication applied the same procedure without additional anodization step.

2.2 Fretting test

To evaluate the wear behavior of screws under fretting, a test rig setup was configured to simulate the shear at bone implant interface with the load applied vertically on screws (see Figure 1). As shown in Figure 1, a load F_N is applied on bone screws. During the fretting,

debris generated and trapped at bone implant interface is illustrated in Figure 1b, Figure 1c. As the micromechanical properties are altered in dehydrated bone, in this study fresh sheep femoral bones were used in this study as our ex−vivo fretting counter for screws, [19]. The middle part of the femoral bone was collected from local abattoir within 2 hours of sacrifice. The screw was inserted in the new fresh bone to form a tight contact between bone and screw interface. Before insertion, a hole with 3mm in diameter was drilled in the center of the bone, and each self-tapping screw was inserted into each femoral bone individually. Fretting motion was examined by SRV-IV oscillating reciprocating friction and wear tester (Nye Lubricants Company). A load with 100 N was applied on screw head with 300 μm fretting distance at 37°C. Fretting was conducted at frequency of 10 Hz and 36×1000 cycles test was performed.

2.3 Biocorrosion characterization

To investigate biocorrosion behavior, an electrochemical workstation CHI660D (CH Instruments, Inc, Shanghai, China) was used to measure the change of open circuit potential (OCP) was achieved in *E* versus time in simulated body fluid solution (SBF). Before the fretting test, the OCP curve was recorded for 1200 seconds until curve stabilized. The comparative analysis was carried out by OCP value after 36×1000 cycles fretting test. Energy dispersive X-ray spectroscopy (EDX) was used to analyze the chemical composition of samples at different areas on specimens.

2.4 Fretting track observation

2.4.1 Optical examinations

Optical observation is an intuitive and widely applied method to evaluate severe wear or corrosion for orthopaedic retrieval implants analysis. As the dark green color of nanotubes layer is significantly different with titanium alloy burnished surface, optical investigations can be a useful tool to investigate the general fretting of the three samples.

2.4.2 Wear observation at tapping areas

According to shear stress generated during insertion, which concentrates at the thread ridge areas of the screw, where the most damaged occurred during insertion by countering the bone. The repetitive shear stress can weaken the bonding of the TiO_2 nanotube layer and lead to TiO_2 nanotubes debonding from the screw substrate. Therefore, the tapping areas of three samples were examined by SEM, and the nanotubes integrity on NT and SONT screws were

investigated and compared. A FESEM (JEOL-7601F, JEOL, Japan) was operated at voltage of 5 kV for topography observation of screws before and after fretting test. The topography of MA, NT and SONT were examined and compared under the same magnification. Under the selected tapping areas, nanotubes damage on NT and SONT could be compared obviously.

2.4.3 NT and SONT integrity on the thread ridges

Ascribed to the scale of nanotubes, conventional wear quantitative methods, for example weight loss is not a suitable method to measure the fretting wear of the nanotubes. Further, wear damage of the screw surface could be widely occurred on different locations of whole screw. Herein, a methodology was proposed to quantify nanotubes damage on NT and SONT screws.

Figure 2 illustrates the locations observed by SEM on the self-tapped screw. The damage of nanotubes was mainly concentrated on thread ridge at points 1, 2, 3, 4 and 5 on the thread. The five points were defined as the areas passed through the central line of the screw (the line passing along the drill tapping plane) and the proportion of debonding areas were measured by Image J software 1.47 V (National Institutes of Health). Under SEM scanning area in every location (1.01×10.1 mm^2), the actual nanotubes debonded areas (see Figure 2) were calculated. With the average actual lift off areas value of five points, one circle of thread lift off area (φ) can be calculated by Equation 1, based on the hypothesis that the wear debonding areas was equal on different regions on thread.

$$\varphi = \frac{\frac{(a_1+a_2+a_3+a_4+a_5)}{5}}{\frac{1.01}{2\pi r}} \quad (1)$$

Where, φ is the lift off area on one circle of thread, mm^2; a_i (i=1, 2, 3, 4, 5) is each observation points of actual nanotubes lift off area, mm^2; r is the major radius of thread with 1.75 mm. Statistical analysis of volume loss was performed by one-way ANOVA.

However, the method above described is unable used to work out the debonding area of MA sample as no TiO_2 nanotube layer on the MA screw, as such the damage areas could not be determined by SEM observation. Therefore, the fretting of titanium screw (MA sample) was only topographically compared with NT and SONT screws.

2.4.4 MA, NT and SONT thread width measurement

As insertion procedure generated stress and harsh wear at thread ridge, the tips were

damaged more than other locations, the material on thread tip would be mechanically removed. Therefore, worn threads become thicker than pristine thread, MA, NT and SONT thread width were measured by SEM (JEOL-7601F, JEOL, Japan) and ImageJ 1. 47V (National Institutes of Health) was carried out to measure the width of thread after the fretting test.

3. Results

3.1 TiO_2 nanotube layer

NT and SONT exhibited a optical homogeneous dark green color without obvious defects. The micro topography of MA, NT and SONT are shown in Figure 3. It was observed from the SEM examination that the machined groove track displayed a rough topography under micro scale on MA screw. In contrast, there were non-machining grooves on both NT and SONT specimens. However, vertically arranged nanotubes structure on NT and SONT were observed. Micro/submicro sized pits were formed on both NT and SONT layers.

Figure 4. shows the high resolution of SEM examinations of both NT and SONT screws. It was observed that the nanotube diameters of both NT and SONT were 100 nm in average, with a length (nanotubes layer thickness) of 2.5±1 μm. SONT exhibited a 120-150 nm thick bonding layer at nanotubes bottom, whereas NT exhibits a typical nanotubes spherical bottom. The SEM examinations revealed the shape of pits varies, and distributed randomly within both NT and SONT layers, the details of pits are shown in Figure 4a1.

Meanwhile, the chemical compositions of both NT and SONT at the pit areas were examined by EDX and were shown in Figure 5. It was observed that the chemical composition of nanotubes of both NT and SONT exhibited 56-57% of oxygen and 23-24% of titanium, indicates TiO_2 composition. However, the NT pits areas presented 54% titanium, 21% fluorine and no oxygen was detected. While as the elements on SONT pits areas showed high similarity with that on nanotubes areas. Based on results, it is speculated that chemical composition of pits on NT was titanium substrate, and fluorine concentrated at the pits area.

3.2 Corrosion behavior of MA, NT and SONT modified screws

Before fretting, the OCP of both SONT and MA screws were stabilized at - 0.17V *vs.* SCE, exhibited low tendency to corrosion (Figure 6a). By contrast, NT presented the lowest OCP value with - 0.28V *vs.* SCE. The results are in contrary with the previous studies of anodization on pure titanium [20]. The reason responsible for this can be attributed to the anodization in

NH_4F undermined the pristine machinery titanium surface, led to a lower OCP value. Impressively, as the presence of bonding layer, SONT proved highest corrosive resistance, as indicated OCP value.

After fretting test, the worn screws were immersed in fresh SBF. Both NT and SONT screws displayed decreased OCP values. Interestingly, remarkable decrease of the OCP value was observed on Ma screw. As the natural titanium oxide is mechanically depassivated during fretting (or removal during insertion), the titanium substrate of Ma screw exposed into corrosive environment, leading to decreased OCP value from -0.17V to -0.36V *vs.* SCE, with 0.19V *vs.* SCE decreased value (see Figure 6b.). In contrast, the decreased OCP value of NT was only approximately 0.04V *vs.* SCE, from -0.29V to -0.33V *vs.* SCE. Meanwhile, the SONT was decreased around the same value, 0.05V *vs.* SCE from -0.17V to -0.22V *vs.* SCE. However, SONT exhibited the highest value of OCP even after fretting, indicating the mechanical stability of SONT bonding layer to protect titanium against corrosion.

3.3 Fretting track observation

3.3.1 Optical general investigation

Optical images demonstrated that the most of nanotube film on both NT and SONT were maintained and no severe damage was observed during the fretting test, as revealed in Figure 7. However, obvious debonding that exposed the alloy substrate were observed mainly at thread ridge. There has no obvious worn marks on the thread ridge bottom. Obvious substrate exposure was also detected at the tapping areas on both NT and SONT screws as shown in Figure 7b2 and 7b3, respectively. Moreover, nanotubes on NT threads ridge have deboned, whereas the nanotubes on SONT were less damaged.

3.3.2 Fretting Wear evaluation at tapping areas

Figure 8 illustrates the worn marks of the drill tapping areas on three screws worn, suggesting the tapping areas may have been possibly damaged during the insertion. Figures b1 and c1 illustrate that patches of the nanotubes on NT and SONT screw tapping areas were debonded. In contrast, b2 and c2 have shown that the nanotubes layer on SONT was more integrated as it remained in the same area. On tapping plane, NT screws exposed more substrate areas than that of SONT (Figure 8b1, b2, c1 and c2, white arrow). MA surface has been worn on areas due to the presence of surface asperity. Figure a1 and a2 demonstrate that

the worn on MA screw was heavy, scathes were widely distributed on tapping areas. Ascribed to the presence of nanotubes, NT and SONT screws surfaces displayed a slight worn than MA screw.

3.3.3 NT and SONT integrity on thread ridge

As shown in Figure 9 (MA 1-5), the MA screw thread ridge was worn heavily. Apart from thread worn, the damage was also remarkable on areas both above and beneath the threads. However, severe wear on NT and SONT were not obvious, as revealed in Figure 9. This may attribute to the presence of protective nanotubes layer. Worn areas of NT and SONT screws were mainly distributed adjacent the thread ridge as observed in Figure 9. It was also observed that all the nanotubes layer on five thread ridges (from NT-1 to NT-5) were removed from the substrates. Furthermore, areas near the thread tips were also observed delaminated from the substrate and led to the exposure of the substrate (see Figure 9 NT-2, NT-3 and NT-4, white arrow). It is postulated that SONT exhibited an improved mechanical stability, as confirmed by the observation that the nanotubes remained even in some thread areas (SONT-2 and SONT-5, black arrow). Moreover, some areas of destroyed nanotubes displayed light gray (different with the substrate), indicating that the bonding layer still covered the titanium substrate (SONT-1 to SONT-5, red arrow).

Use the methodology of deboned nanotubes quantitative analysis illustrated in Equation 1, the deboned areas on every thread of NT and SONT were calculated. Figure 10 shows the debonding areas on one thread (φ) of NT and SONT screw thread tip. As the p value was 0.0051, SONT sample exhibited an average debonding areas of 0.23 mm^2 while it was 0.36 mm^2 for NT sample. As calculated, the debonded areas on thread of the SONT decorated screw decreased ~36.11% compared with NT screw, indicating an improved anti-fretting wear for SONT nanotubes layer. Especially, among the five SEM selected points, it was noted that SONT-5 had a lowest worn of only 0.06mm^2.

3.3.4 MA, NT and SONT screw thread worn width measurements

Figure 11 illustrates the selective measurement points (marked with 1, 2 and 3) on worn thread tracks of MA, NT and SONT screw. It was revealed that the MA screw displays the highest value of thread width, with 172.13 μm in average, NT screw reached 154.81 μm and 121.25 μm for the SONT screw (Figure 12). Static analysis shows significant difference

between width of NT thread and that of MA with p=0.036, and the p value of NT width with SONT width is 0.0072. The SONT screw thread width is minimum worn, with the narrowest thread worn track after fretting test.

4. Discussion

Implants with appropriate initial contact to adjacent bone generate physical stress at the interface, while the shear generates relative micromotions. The continuous micromotion combined with biological corrosion (fretting corrosion) generates foreign debris, which is the main cause for chronic inflammatory and/or aseptic loosening [21-24]. Although the NT and SONT were successfully generated on TC4 medical screws, micro pits were observed on both surfaces, which was most likely due to erosion of the vanadium oxide during the anodization in fluorine containing electrolyte [6, 25]. The EDX examination well proved the presence of bonding layer at micro pits areas. On nanotubes areas, both NT and SONT contained above 55% of oxygen, 23-25% of titanium, 10% fluorine, 7-8% carbon and less than 3% vanadium, as reported in Figure 5. However, the chemical composition in pits area shows a significant difference. For the pits on NT screw contain 54% titanium, 21% fluorine, 17% carbon, 5% aluminum and 3% vanadium, indicating the composition of alloy substrate without the presence of large amount oxides. Furthermore, the fluorine contains was two folds higher than that of nanotubes areas. Due to selective dissolution during anodization, the phase contains vanadium (β phase) was enhanced with etching in fluorine containing electrolyte, due to the high solubility of vanadium oxide [25]. The chemical composition of pits on SONT contain same amount of oxygen, titanium, fluorine compares with nanotubes areas, confirming a layer of titanium oxides was formed at pits areas.

The lower OCP value of NT on Ti6Al4V was due to the micro pits formed during anodization. The formed pits were 'channels' linking corrosive biofluid to substrate while immersed in SBF environment, leading to NT surface corrosion. The improvement of corrosion resistance of SONT was due to introduce of bonding layer at the interface of nanotubes and alloy substrate. From the initial OCP value of SONT, the bonding layer sealed the micro pits at bottom of nanotubes to obstruct the aforementioned 'channels' (Figure 13).

The presence of interfacial bonding layer not only improved corrosion resistance, but also enhanced the tribological performance of SONT layer. Orthopaedic screws can be even

damaged both during the insertion procedure and by long-term fretting *in vivo*. As self-tapping screw's thread faces with mass stress and heavy rubbing during drilling and installation, the cortical bone can mechanically remove the material on the thread ridge. From the comparison SEM images of the tapping areas, SONT has the minimum debonding areas.

After insertion, due to the full mechanical contact at bone-thread interface, threads tips have a more severe fretting in some areas than others. The SONT exhibited 40% less of nanotubes debris released than that of NT. Although the damage was only at μm^2, detached nanotubes from substrate might generate a micro sized cluster that would release into the bone and cause tissue reactions. In vivo tissue reactions for TiO_2 nanotubes are still barely studied, nevertheless the micro-sized wear debris released in tissue have been widely proven to be toxic.

Furthermore, nanotubes as a layer of TiO_2 covers alloy substrate and plays a vital role in protecting titanium implant, thus any NT detachment leads to expose the substrate directly into the biocorrosive liquid in vivo atmosphere, leading to metal ions released from the areas. Moreover, the experimental results of thread width of three screws also proved the SONT had the highest capability to protect worn thread, as debris generated could be easily trapped at interface.

5. Conclusion

The NT and SONT were generated on medical grade Ti_6Al_4V (TC4) screws to fabricate TiO_2 nanotube-decorated bone fixation. The fretting and corrosion behavior of the modified screws were investigated by an *ex-vivo* bone screw fretting simulation system and OCP measurement carried out in SBF. The results demonstrated that the screw decorated with SONT exhibits the potential to be applied on orthopaedic devices. The conclusion can be drawn as follows:

1. Before fretting test, the OCP value of NT was lower (-0.29V) than that of Ma surface (-0.17V), indicates that NT on alloy has more tendency to erosion. However, the present of NT film protected the titanium substrate during fretting process as OCP decreased only 0.04V. Impressively, OCP of MA screw decreased significant after fretting (decreased 0.19V), exhibited a poor mechanical stability of bare alloy surfaces.

2. SONT displayed the highest OCP value both before (-0.17V) and after fretting (-0.22V).

Impressively, the OCP value of SONT after fretting was still higher than that of the NT before fretting.

3. TiO_2 nanotubes layer has well proved its protective function against fretting damage on NT and SONT screws, both screws ridges have significantly less worn than Ma screw.

4. SONT exhibited significantly enhanced fretting resistance than NT. Thus, SONT displays an enhanced fretting resistance compared to NT and Ma screws.

Acknowledgement

This work is financially supported by the EU via the H2020-MSCA-RISE-2016 program (734156), Royal Society via the International Exchange Program (IE161349), Key Research Project from the National Key Research and Development Program of China (2016YFC1100401), National Natural Science Foundation of China (51705507), and Young Elite Scientists Sponsorship Program by CAST (2017QNRC0181).

References:

[1] M. Geetha, A.K. Singh, R. Asokamani, A.K. Gogia, Ti based biomaterials, the ultimate choice for orthopaedic implants - A review, Prog Mater Sci, 54 (2009) 397-425.

[2] I.S. Park, T.G. Woo, W.Y. Jeon, H.H. Park, M.H. Lee, T.S. Bae, K.W. Seol, Surface characteristics of titanium anodized in the four different types of electrolyte, Electrochim Acta, 53 (2007) 863-870.

[3] S. Oh, C. Daraio, L.H. Chen, T.R. Pisanic, R.R. Finones, S. Jin, Significantly accelerated osteoblast cell growth on aligned TiO2 nanotubes, J Biomed Mater Res A, 78A (2006) 97-103.

[4] C. von Wilmowsky, S. Bauer, S. Roedl, F.W. Neukam, P. Schmuki, K.A. Schlegel, The diameter of anodic TiO2 nanotubes affects bone formation and correlates with the bone morphogenetic protein-2 expression in vivo, Clin Oral Implan Res, 23 (2012) 359-366.

[5] N. Swami, Z.W. Cui, L.S. Nair, Titania Nanotubes: Novel Nanostructures for Improved Osseointegration, J Heat Trans-T Asme, 133 (2011).

[6] K. Lee, A. Mazare, P. Schmuki, One-Dimensional Titanium Dioxide Nanomaterials: Nanotubes, Chem Rev, 114 (2014) 9385-9454.

[7] H.R. Li, Q. Cui, B. Feng, J.X. Wang, X. Lu, J. Weng, Antibacterial activity of TiO2 nanotubes: Influence of crystal phase, morphology and Ag deposition, Appl Surf Sci, 284 (2013) 179-183.

[8] Y. Zhao, Q. Xing, J. Janjanam, K. He, F. Long, K.B. Low, A. Tiwari, F. Zhao, R. Shahbazian-Yassar, C. Friedrich, T. Shokuhfar, Facile electrochemical synthesis of antimicrobial TiO2 nanotube arrays, Int J Nanomed, 9 (2014) 5177-5187.

[9] N. Wang, H.Y. Li, W.L. Lu, J.H. Li, J.S. Wang, Z.T. Zhang, Y.R. Liu, Effects of TiO2 nanotubes with different diameters on gene expression and osseointegration of implants in minipigs, Biomaterials, 32 (2011) 6900-6911.

[10] L. Salou, A. Hoornaert, G. Louarn, P. Layrolle, Enhanced osseointegration of titanium implants

with nanostructured surfaces: An experimental study in rabbits, Acta Biomater, 11 (2015) 494-502.
[11] S. Bauer, J. Park, K. von der Mark, P. Schmuki, Improved attachment of mesenchymal stem cells on super-hydrophobic TiO2 nanotubes, Acta Biomater, 4 (2008) 1576-1582.
[12] F. Schmidt-Stein, S. Thiemann, S. Berger, R. Hahn, P. Schmuki, Mechanical properties of anatase and semi-metallic TiO2 nanotubes, Acta Mater, 58 (2010) 6317-6323.
[13] D.A. Wang, B. Yu, C.W. Wang, F. Zhou, W.M. Liu, A Novel Protocol Toward Perfect Alignment of Anodized TiO2 Nanotubes, Adv Mater, 21 (2009) 1964-1967.
[14] O. Bostman, H. Pihlajamaki, Clinical biocompatibility of biodegradable orthopaedic implants for internal fixation: a review, Biomaterials, 21 (2000) 2615-2621.
[15] S.B. Goodman, Z.Y. Yao, M. Keeney, F. Yang, The future of biologic coatings for orthopaedic implants, Biomaterials, 34 (2013) 3174-3183.
[16] M. Sundfeldt, L. V Carlsson, C. B Johansson, P. Thomsen, C. Gretzer, Aseptic loosening, not only a question of wear: a review of different theories, Acta Orthop, 77 (2006) 177-197.
[17] C.E.B. Marino, L.H. Mascaro, EIS characterization of a Ti-dental implant in artificial saliva media: dissolution process of the oxide barrier, J Electroanal Chem, 568 (2004) 115-120.
[18] I. Hacisalihoglu, A. Samancioglu, F. Yildiz, G. Purcek, A. Alsaran, Tribocorrosion properties of different type titanium alloys in simulated body fluid, Wear, 332 (2015) 679-686.
[19] J.Y. Rho, G.M. Pharr, Effects of drying on the mechanical properties of bovine femur measured by nanoindentation, Journal of materials science. Materials in medicine, 10 (1999) 485-488.
[20] W.Q. Yu, J. Qiu, L. Xu, F.Q. Zhang, Corrosion behaviors of TiO2 nanotube layers on titanium in Hank's solution, Biomed Mater, 4 (2009).
[21] S.B. Goodman, Wear particles, periprosthetic osteolysis and the immune system, Biomaterials, 28 (2007) 5044-5048.
[22] J. Geringer, B. Forest, P. Combrade, Fretting-corrosion of materials used as orthopaedic implants, Wear, 259 (2005) 943-951.
[23] S. Barril, N. Debaud, S. Mischler, D. Landolt, A tribo-electrochemical apparatus for in vitro investigation of fretting-corrosion of metallic implant materials, Wear, 252 (2002) 744-754.
[24] J. Raphel, M. Holodniy, S.B. Goodman, S.C. Heilshorn, Multifunctional coatings to simultaneously promote osseointegration and prevent infection of orthopaedic implants, Biomaterials, 84 (2016) 301-314.
[25] J.M. Macak, H. Tsuchiya, L. Taveira, A. Ghicov, P. Schmuki, Self-organized nanotubular oxide layers on Ti-6Al-7Nb and Ti-6Al-4V formed by anodization in NH4F solutions, J Biomed Mater Res A, 75 (2005) 928-933.

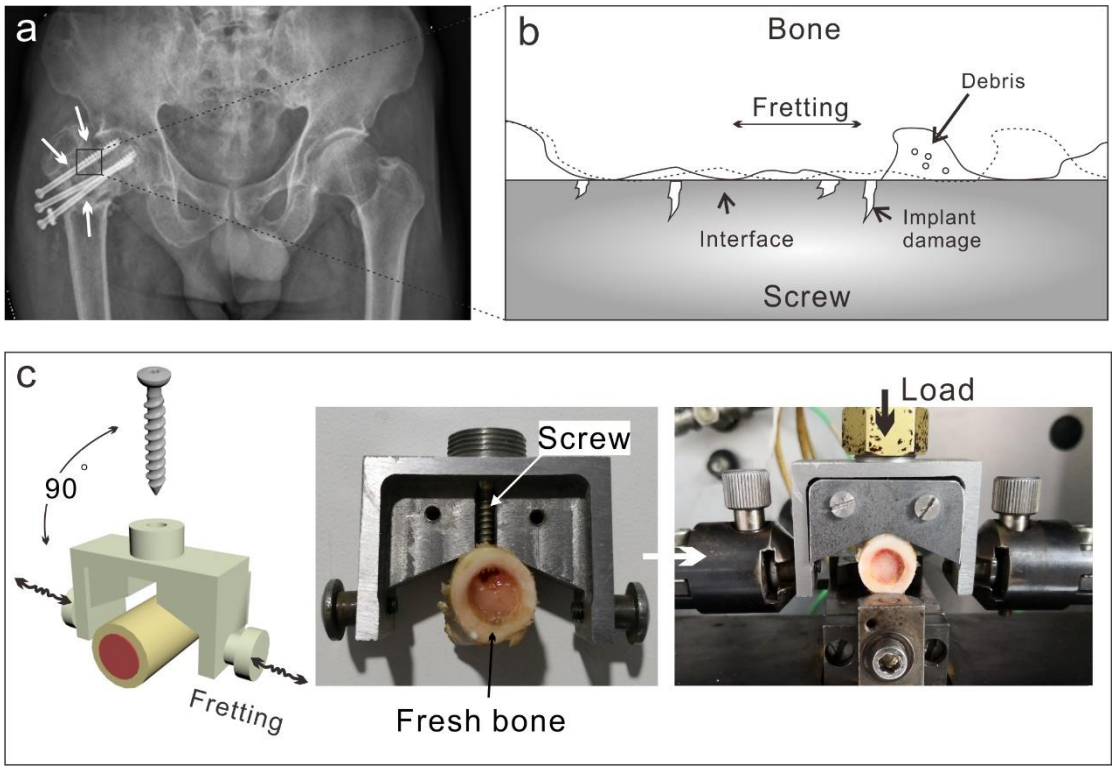

Figure 1. Schematic of fretting at bone-implant interface: Fretting behavior of inserted injury fixation screws (a), load vertically applied on screws, fretting behavior at bone implant interface, the fretting leads to implant surface damage and wear debris generation (b) and mechanical jig setup (c)

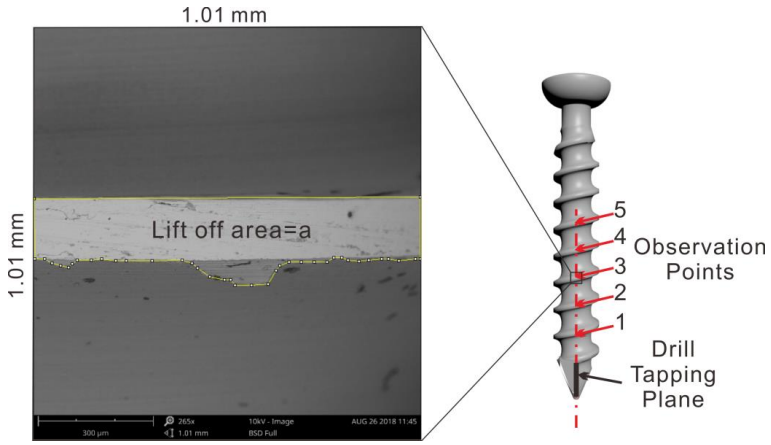

Figure 2. Schematic of self-tapping screw and SEM observation of debonding of TiO_2 nanotube layer, five points on the thread ridge were used for SEM examinations.

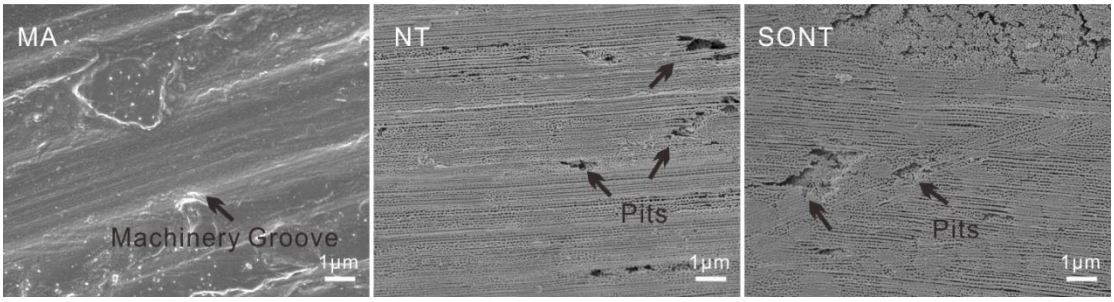

Figure 3. FESEM images of the surfaces of MA, NT and SONT screws. The micro pits were formed on both NT and SONT surface (black arrows).

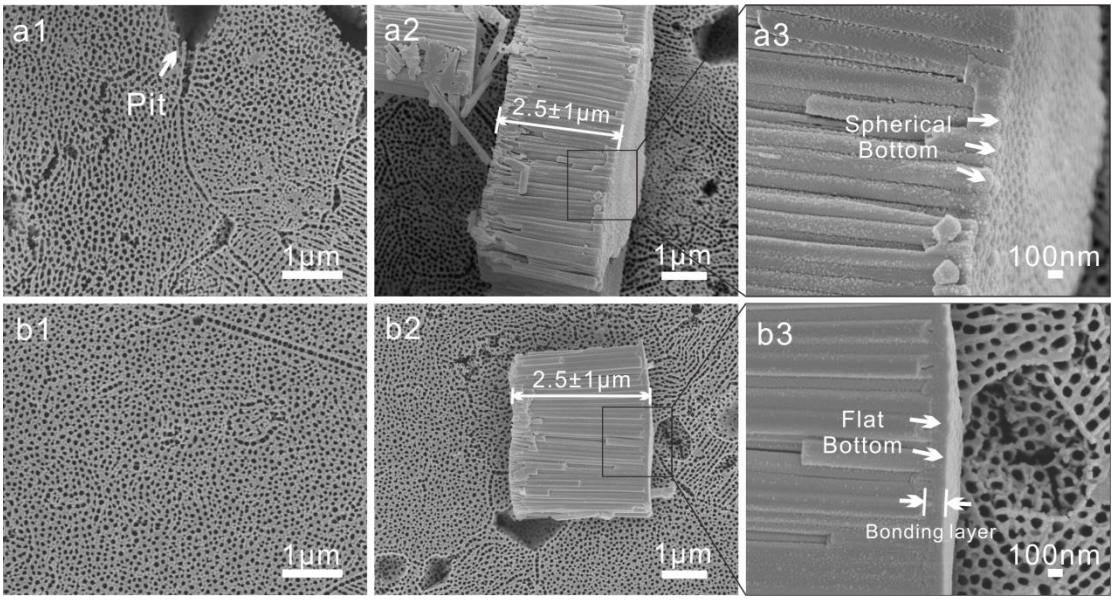

Figure 4. FESEM images of NT and SONT, top view of NT (a1) and SONT (b1), side view of NT (a2) and SONT (b2) and the bottom part view NT (a3) and SONT (b3). The structure of NT and SONT were shown highly similarity except the bottom, a flat layer was bonded nanotubes bottom in SONT.

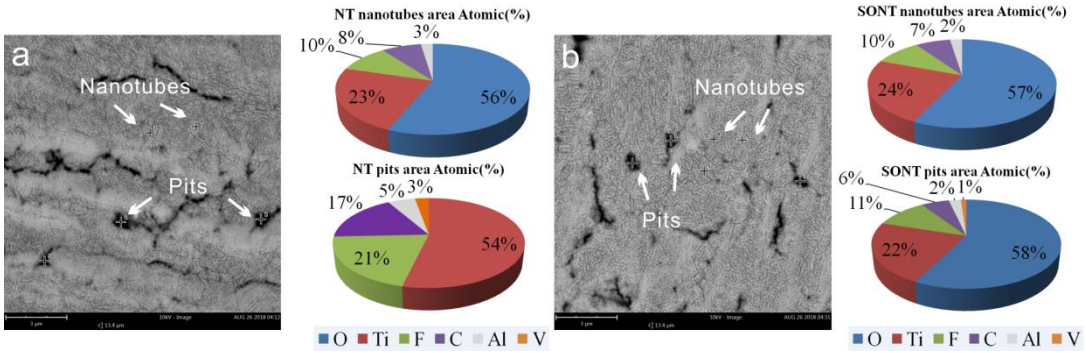

Figure 5. SEM-EDX images of NT and SONT at pits and nanotubes areas: NT pits areas and nanotubes areas (a) and SONT pits areas and nanotubes areas (b).

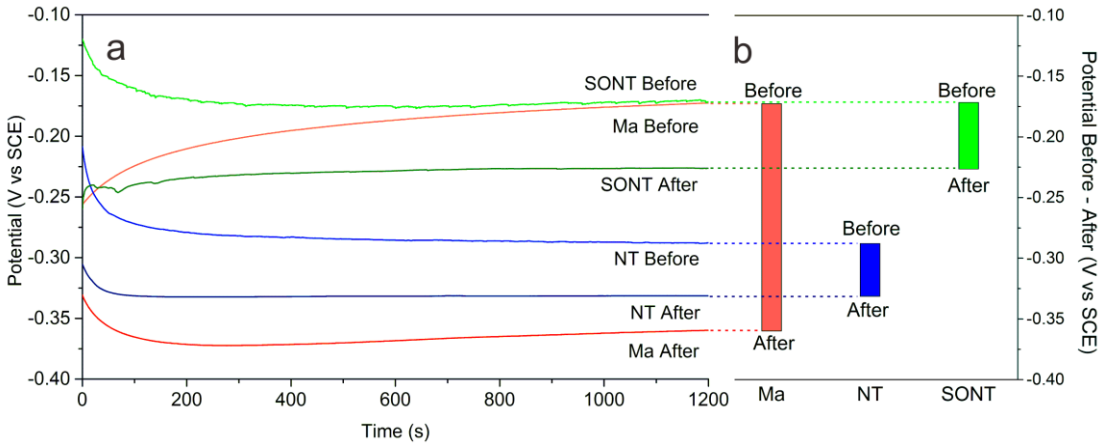

Figure 6. Open circuit potential of MA, NT and SONT: before and after fretting (a) and OCP decreased value of each screws after fretting (b).

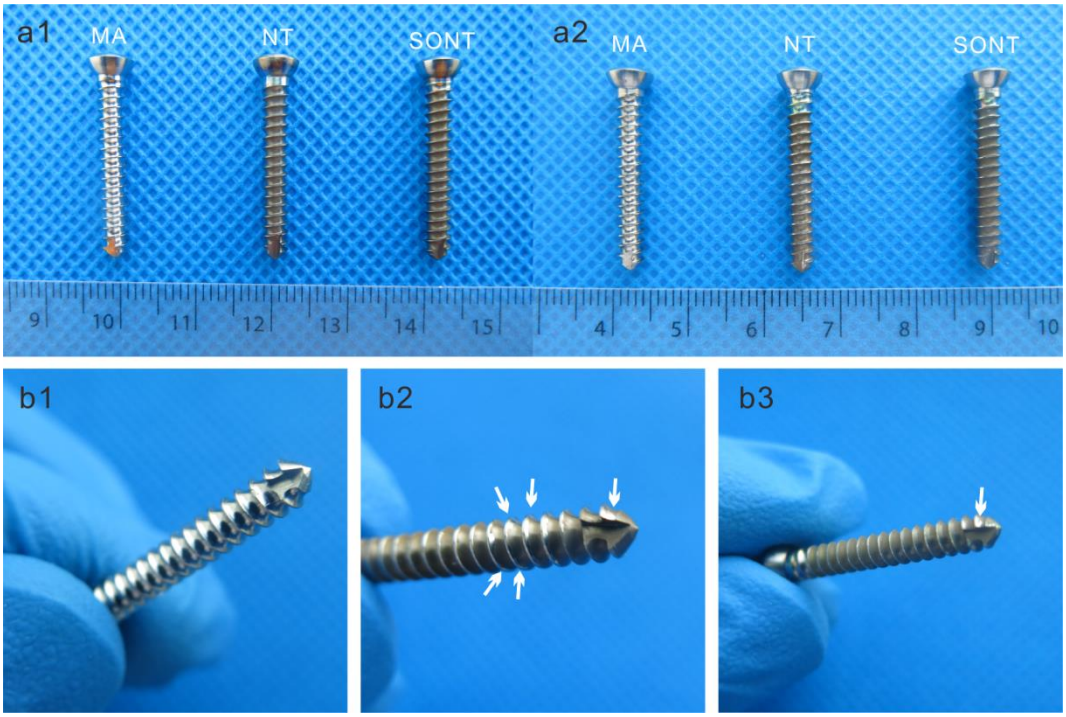

Figure 7. Optical image of MA , NT and SONT screws before fretting test (a1) and after fretting test (a2). The enlarged optical images revealed the fretting worn markers on pristine (b1), NT (b2) and SONT (b3) screws, respectively.

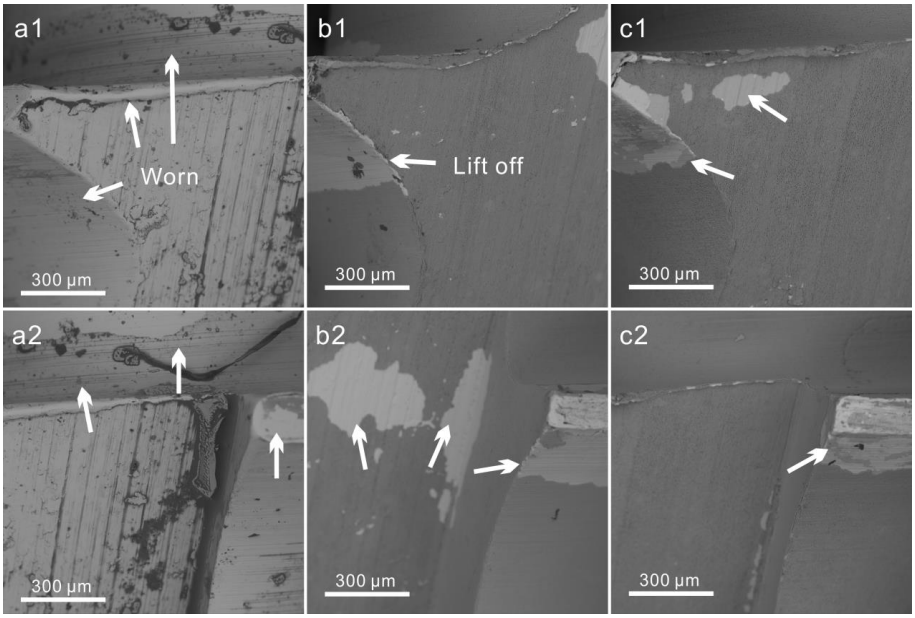

Figure 8. Worn after fretting on drill tapping areas, MA screw a1 and a2, NT screw b1 and b2, SONT screw c1 and c2. MA tapping area has worn heavily, tapping upper areas were also worn (a1 and a2, white arrows). The nanotubes layer lift off on NT tapping areas were more than that on SONT (b1 and c1, b2 and c2), some areas on SONT displayed light grey color (c1 and c2, white arrows).

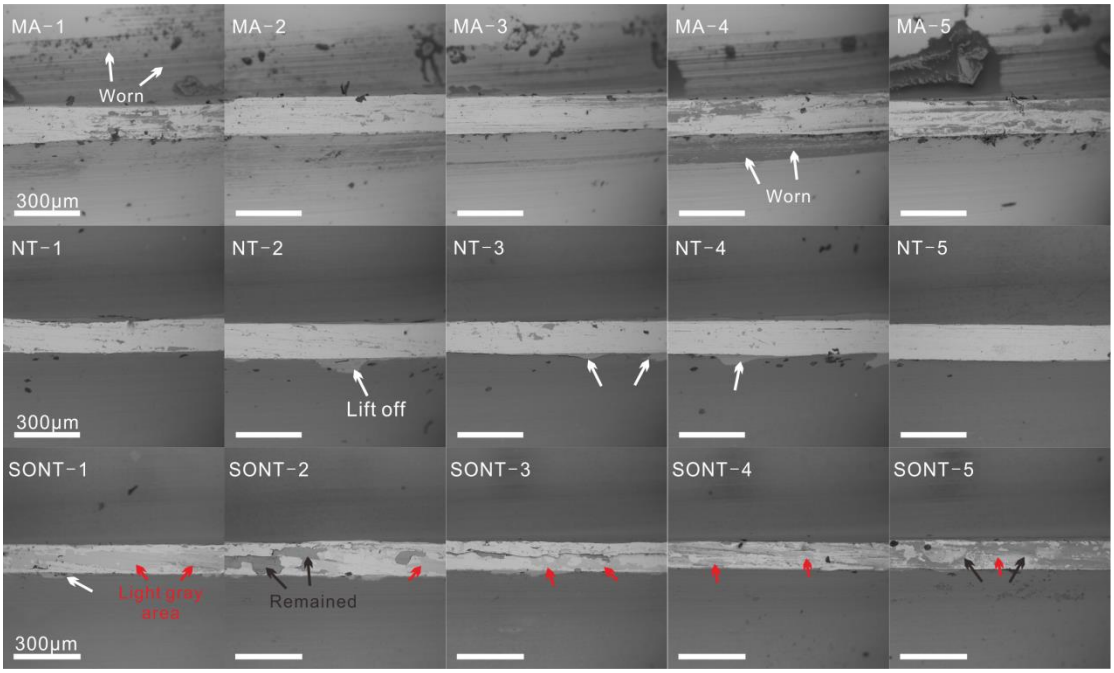

Figure 9. SEM observations of worn thread ridges of machined (Ma 1-5), NT (NT 1-5) and SONT (SONT 1-5) screw, bar=300 µm.

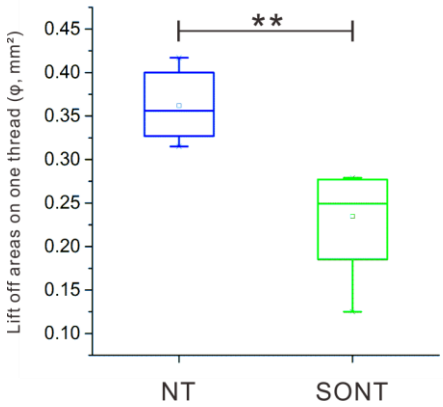

Figure 10. Lift off areas of nanotubes layer on thread for NT and SONT decorated screw, **, $p<0.01$. p value: 0.0051, Error bars represent standard error with the mean (s.e.m).

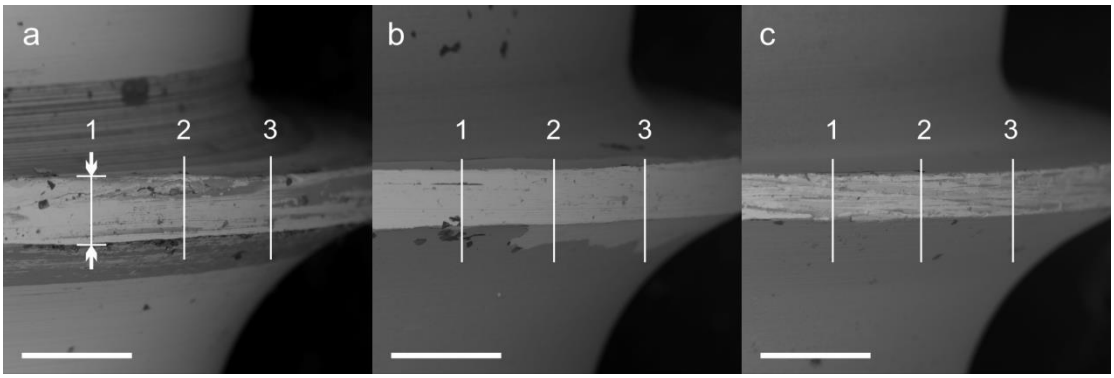

Figure 11. Thread width measure points (white bar areas) of Ma(a), NT(b) and SONT(c), bar=300μm.

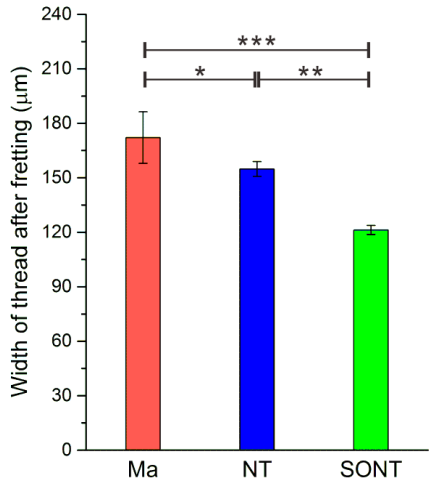

Figure 12. Thread width of Ma, NT and SONT after fretting, *, $p<0.05$, **, $p<0.01$, ***, $p<0.001$.

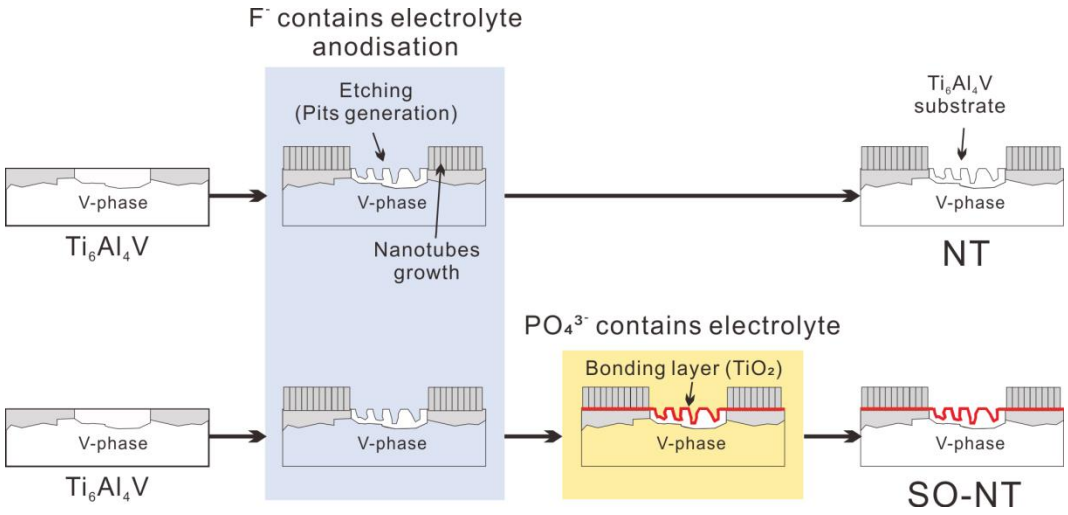

Figure 13. The vanadium containing phase dissolved during nanotubes generation process that caused micro pits formed, leading to substrate exposure. The bonding layer presents a vital role to against corrosion in SBF though sealed the pits.